Measurements of long-term strength changes due to cyclic loading in Gulf of Mexico clay

Fauzan Sahdi
Oceans Graduate School, The University of Western Australia, Perth, WA, Australia & Department of Civil Engineering, Universiti Malaysia Sarawak, Malaysia (on postdoctoral leave)

Joe G. Tom
Oceans Graduate School, The University of Western Australia, Perth, WA, Australia

Noor Laham
University of Bologna, Bologna, Italy

Phil Watson, Fraser Bransby & Christophe Gaudin
Oceans Graduate School, The University of Western Australia, Perth, WA, Australia

ABSTRACT: Many types of deep-water offshore infrastructure are subject to cyclic movements during their design life. It is acknowledged that cyclic movement in normally consolidated clay causes the undrained strength to decrease through remoulding; but the strength can also recover (through reconsolidation) if dissipation of excess pore pressure is allowed to occur. In many offshore environments however, the soil profile is overconsolidated, especially near the mudline – and it is less clear how stress history affects remoulding and reconsolidation behaviour. Furthermore, previous testing to investigate this effect has mostly been conducted in 'laboratory' kaolin clay, and whether these results reflect the behaviour of natural clays is less known. To address these uncertainties, a series of long-term cyclic T-bar tests were performed in samples of reconstituted Gulf of Mexico (GoM) clay prepared at overconsolidation ratios (OCR) of 1 and 10. Episodic cyclic penetrometer tests were performed at peak-to-peak displacement amplitudes of four penetrometer diameters, followed by wait periods of 10 hours in between each episode. This paper confirms that soil strength can increase in normally consolidated natural clay (although the increases are smaller than those seen in kaolin), while also highlighting how the OCR affects the strength changes after reconsolidation is allowed to occur.

Keywords: Gulf of Mexico clays, cyclic loading, T-bar penetrometer, remoulding, reconsolidation

1. Introduction

Geotechnical processes associated with the day-to-day operations of risers and mooring anchors involve cylic loading of varying amplitudes. These cyclic interactions cause the surrounding soil to weaken through remoulding, and this effect is well recognized in offshore design practice [1]. Previous work [e.g. 2] has shown that under scenarios of continuous cyclic loading, the soil may 'heal' and the undrained strength increase. Increases in soil strength are caused by reconsolidation, where generated positive excess pore pressures dissipate, leading to soil densification [3]. The progression and magnitude of strength increase is expected to depend on the type and stress history of the surrounding soil. In this paper, we explore these changes for a reconstituted Gulf of Mexico clay under varying stress histories.

The effect of strength regain and increase in fine grained soils depends on the type of subsea infrastructure considered. For anchors, strength increase implies that the anchor size can be optimised (reduced) if the associated increase in anchor holding capacity can be relied upon. On the other hand, steel risers and well conductors are governed by structural fatigue and hence, an increase in soil strength (and the associated soil-structure stiffness) may exacerbate structural fatigue damage. If strength and stiffness increases do occur, it would be unconservative not to consider them in design; and typical design methods that assume the remoulded riser-soil stiffness may overestimate the steel riser fatigue life, since the stiffness may be underpredicted by a factor of ~ 10 [2]. It is clear that a good understanding of the evolution of soil strength due to long-term environmental and operational cyclic loading is important to optimise the design of various subsea infrastructure.

The effects of remoulding and strength increase through reconsolidation have been demonstrated in kaolin clay through T-bar tests in both the centrifuge and laboratory floor [3, 4]. An example of results from White and Hodder [3] is reproduced in Figure 1. As can be seen in Figure 1(a), the T-bar test was conducted by first penetrating a model T-bar (diameter, D = 5 mm) to a depth of 60 mm. Three episodes of cyclic loading (each with 20 cycles over a depth range of 15 – 60 mm) were conducted. Between succesive episodes, the T-bar remained stationary at a depth of 60 mm for 3.5 hours. This test was conducted under a centrifuge acceleration of 50g in lightly overconsolidated kaolin clay with an OCR ranging from approximately 4 (top of cycle range) to 1.8 (bottom of cycle range). Figure 1(a) shows that the measured undrained strength, s_u, increases throughout the profile after each waiting period. The change in the current undrained strength ($s_{u\text{-}n}$) normalised by that measured during initial penetration ($s_{u\text{-}in}$), $s_{u\text{-}n}/s_{u\text{-}in}$ as the cycle number (n) progresses at a T-bar displacement (Δz) of 2 mm above the T-bar resting depth ($\Delta z = 0.4D$ – see Figure 1(a)) is depicted in Figure 1(b). Here, it can be

clearly seen that both the measured $s_{u\text{-}n}$ during initial extraction and the subsequent 'remoulded' $s_{u\text{-}n}$ after the rest period surpasses that measured in previous episodes.

Previous research on long-term soil strength changes has generally focused on contractile kaolin. From a critical state theory perspective, the soil strength in these cases is expected to increase due to dissipation of positive excess pore pressure because the samples are on the 'wet' side of critical state. However, many offshore environments contain seabed soils that are dilatant due to mechnical overconsolidation; for example, through mass soil removal from submarine slides, such as those found in the Sigsbee Escarpment in the Gulf of Mexico [5, 6]. The response of dilatant soils due to long-term, large-amplitude cyclic loading is uncertain and may inhibit design optimisation of steel risers and anchoring systems in these regions.

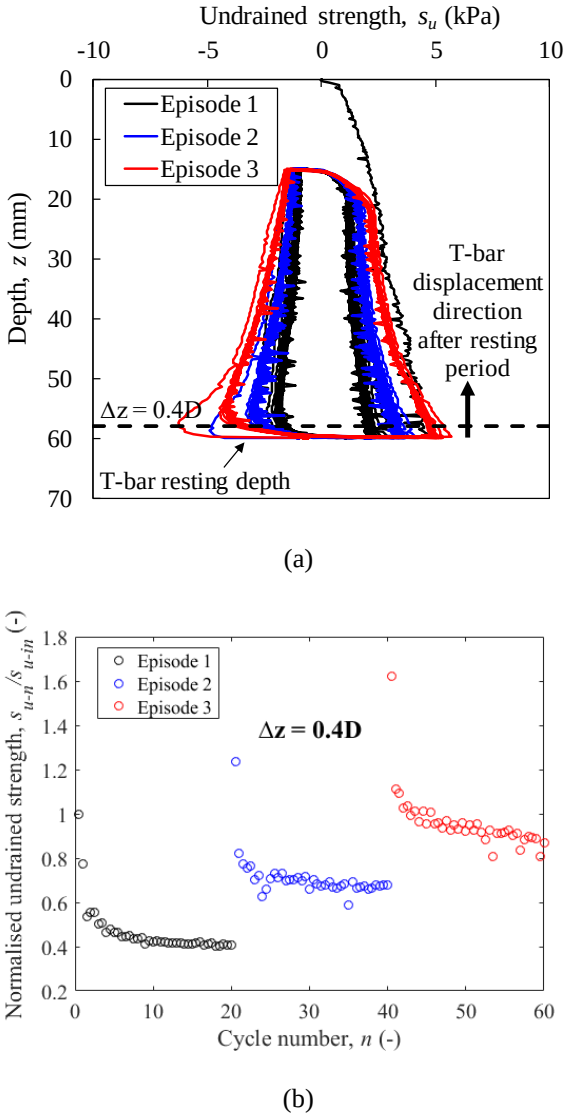

Figure 1. Episodic centrifuge T-bar test in lightly overconsolidated kaolin [3]: (a) undrained strength profile; (b) evolution of current undrained strength normalised by initial undrained strength at 2 mm above the resting depth (Δz = 0.4D; D = 5 mm)

This paper aims to provide a better understanding of how soil stress history affects long-term strength changes in a reconstituted natural clay. The results of episodic cyclic T-bar testing conducted on reconstituted samples of Gulf of Mexico clay with overconsolidation ratios (OCR) of 1 and 10 are reported. This OCR range is thought to bracket the range of typical stress history conditions encountered in most offshore seabed soils.

2. *Compression properties of GoM clay*

The test programme used reconstituted (deepwater) Gulf of Mexico (GoM) clay samples collected using a Jumbo Piston Corer (JPC). The GoM sample has a plastic limit, liquid limit and specific gravity of 26%, 99% and 2.78 respectively.

The consolidation properties of the GoM clay, obtained from Rowe cell tests are depicted in Figure 2. As can be seen in Figure 2(a), parameters e_λ (void ratio on the normal compression line at a vertical effective stress, σ'_v = 1 kPa) and λ (slope of the normal compression line) as well as κ (slope of the unload-reload line) are used to characterise the lines fitted through the one dimensional consolidation data in e - lnσ'_v (e – void ratio) space.

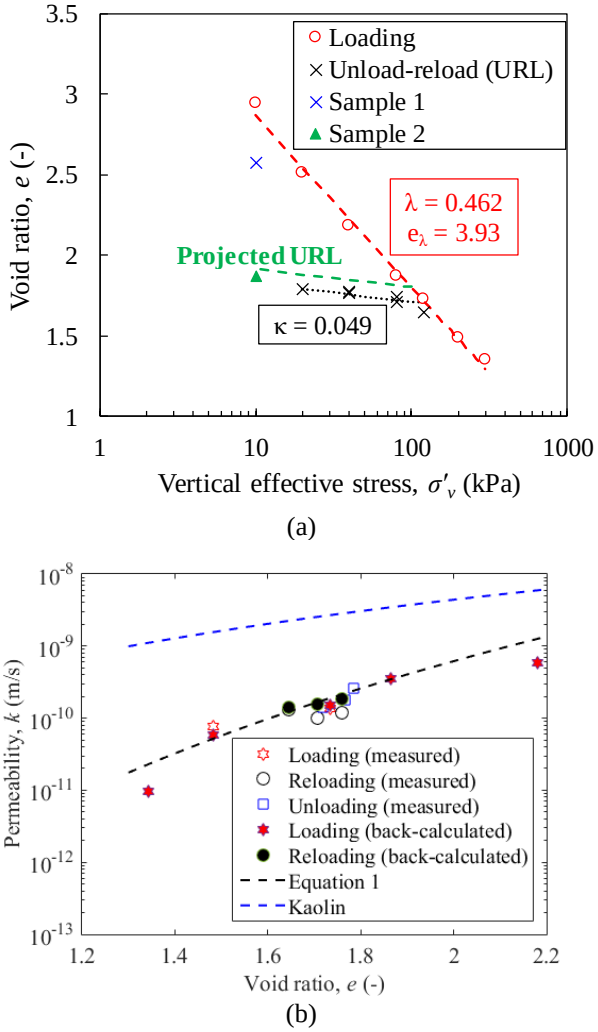

Figure 2. Rowe cell test results: (a) one-dimensional consolidation behavior; (b) permeability

The permeability (k) data measured using the constant head method is depicted in Figure 2(b). The value of k back-calculated from the coefficient of consolidation (c_v), determined using the log-of-time method for all test phases (except during unloading) are also plotted in Figure 2(b). It is evident that the measured and back-calculated k – e data during all the loading and unloading-reloading phases agree well and can be captured via:

$$k = 2 \times 10^{-12} e^{8.27} \text{ m/s} \quad (1)$$

Figure 2(b) demonstrates that the change in permeability of reconstitued GoM clay is mainly a function of the change in e as reported in kaolin clay [7]. The permeability-void ratio trend line for kaolin clay used in the White and Hodder [3] centrifuge T-bar tests, is also included in Figure 2(b). It is evident here that the permeability of kaolin is higher that that of GoM clay, especially at low void ratios, and may be attributed to the higher silt-size content in kaolin.

3. Sample preparation and test equipment

Figure 3 depicts the laboratory test setup where two GoM clay samples were prepared. In each sample, steel plates were used to maintain a constant overburden pressure throughout the test programme.

The GoM test samples were first mixed with water to achieve a water content of 160% (~ 1.6 times the liquid limit) in a large mechanical mixer for two days to ensure a homogeneous slurry. The slurry was then transferred to two strongboxes, each with a dimension of 390 mm (width) × 650 mm (length) × 325 mm (height) on a 25 mm sand layer underlying a layer of geotextile for bottom drainage. Another layer of geotextile was then placed on top of each sample to facilitate top drainage (see Figure 3). The two samples were subjected to different stress histories in order to achieve the desired overconsolidation ratios (OCR) of 1 and 10.

In Sample 1 (OCR = 1), steel plates were placed on top of the slurry to achieve an overburden stress of 10 kPa. These steel plates were placed incrementally to ensure that the sample top layer was competent enough to carry the imposed load without being squeezed from the plate sides. After placement of all steel plates, the settlement of Sample 1 was monitored until primary consolidation was achieved (~ 30 days).

The soil in Sample 2 (OCR = 10) was first loaded to 100 kPa in a hydraulic press for ~ 21 days until primary consolidation was achieved. Similar to Sample 1, steel plates (equivalent to 10 kPa overburden stress) were then placed on top of Sample 2 and the sample was then allowed to swell for 14 days to achieve OCR = 10.

Extensive T-bar testing, using a model T-bar with diameter (D) of 5 mm and length (L) of 20 mm (consistent with that used in White and Hodder [3]), was conducted through 30 mm diameter openings in the steel plates, as depicted in Figure 3. This paper reports selected test results from the more extensive T-bar testing programme. For both Sample 1 and Sample 2, displacement-controlled T-bar cyclic episodes were conducted with each episode comprising 20 cycles with peak-to-peak displacement distances of 20 mm or z/D = 4 (z - T-bar depth below soil surface; D – T-bar diameter) – see Table 1. Before comencement of each T-bar test, the top geotextile layer was trimmed to allow entry of the T-bar into the sample. At the end of each episode, the T-bar remained stationary at the centrepoint of the cycles for 10 hours until the next episode of cyclic T-bar displacements. The number of cycles of the two T-bar tests conducted in Samples 1 and 2 are depicted in Table 1. A vertical-horizontal actuator (see Figure 3) was used to position the T-bar and actuate vertical motion during penetration and extraction at a velocity (v) of 1 mm/s for all the tests reported in this paper. This is equivalent to vD/c_v ratios (c_v – coefficient of consolidation) of ~ 160 and 300 for Samples 1 and 2 respectively, which is sufficient to maintain undrained conditions as the T-bar passes through a given soil horizon [8, 9].

After completion of all T-bar tests, moisture content cores were taken and the average sample void ratios for the two samples calculated from the moisture content data are plotted in Figure 2(a). The measured void ratios are reasonably close to that on the one dimensional normal compression and unload-reload lines.

4. Episodic cyclic T-bar results

The overall results of the episodic cyclic T-bar testing in Sample 1 (OCR = 1) and Sample 2 (OCR = 10) are depicted in Figure 4(a) and Figure 4(b), respectively. The figures present the T-bar resistance profiles in terms of inferred undrained shear strength values (s_u), where s_u was calculated from the resistance force divided by the projected area of the T-bar and a bearing factor, $N_{T\text{-}bar}$ = 10.5, which is based on a full-flow mechanism around deeply embedded partially rough cylindrical object [10, 11].

In both cases, the first episode was preceeded by monotonic penetration, which gave broadly constant undrained strength profiles with depth. The s_u normalised by the effective vertical stress, σ'_v for Sample 1 is ~ 0.27. The monotonic s_u profile in Sample 2 is compared in Figure 4(b) with estimates from the SHANSEP approach [12]:

$$s_u = \sigma'_v \left(\frac{s_u}{\sigma'_v}\right)_{nc} OCR^{\Lambda} \quad (2)$$

Table 1. T-bar test programme

Sample	Number of episodes	Number of cycles per episode	Total reconsolidation time between episodes (hours)	Velocity (mm/s)
Sample 1 (OCR = 1)	5	20	10	1
Sample 2 (OCR = 10)	3	20	10	1

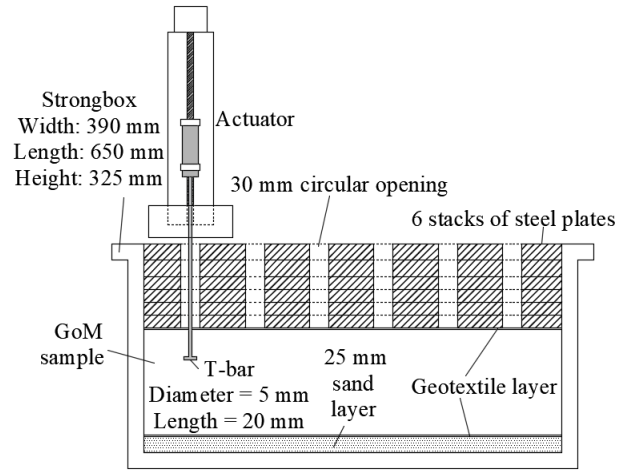

(a)

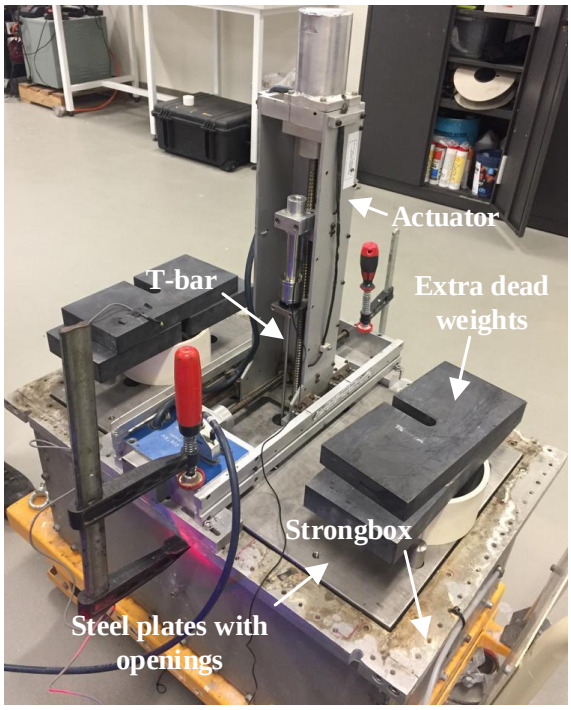

(b)

Figure 3. 1g test arrangement: (a) test schematic; (b) test setup photo

where $(s_u/\sigma'_v)_{nc}$ is the normally consolidated undrained strength ratio, taken as 0.27 based on Sample 1 and Λ = 0.76, selected to provide the best match with the data. This Λ value is ~ 15% smaller than that calculated from critical state theory ($\Lambda = 1 - \kappa/\lambda = 0.894$). However, both $(s_u/\sigma'_v)_{nc}$ and Λ obtained in this test programme are consistent with regional experience and with those for other clays [13].

Figure 4(a) qualitatively indicates that for Sample 1 (OCR = 1), the initial strength measured upon re-penetration in the first cycle (after a rest period of 10 hours) of each subsequent episode appears to increase and is only marginally smaller than that measured in the initial penetration. The post-wait strength profile measured in the first cycle of later episodes generally decreases as the T-bar moves away from the T-bar resting position (z/D ~ 20.4 and z/D ~ 19.4 for Samples 1 and 2, respectively; z – depth below mudline). Closer inspection of Figure 4(a) indicates that the remoulded strength increases in subsequent episodes relative to the first episode.

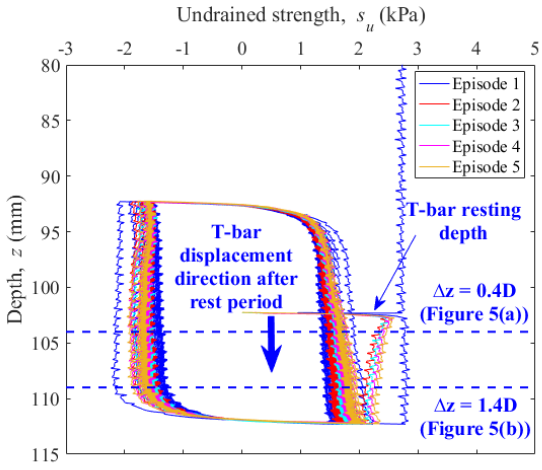

(a)

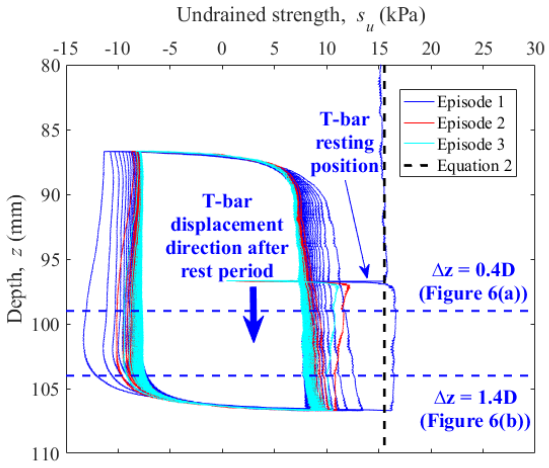

(b)

Figure 4. Undrained strength profile in: (a) Sample 1 (OCR = 1); (b) Sample 2 (OCR = 10)

For Sample 2 (Figure 4(b)), the broad shape of the cyclic episodes are similar to Sample 1, but there is no apparent increase in remoulded strength with episodes. The inital post-wait strengths also reduce with increasing number of episodes, in contrast to Sample 1. This means that the first cycle strength in episode 3 is lower than that in episode 2.

These general findings are further quantified in Figures 5 and 6, which show the evolution of the normalised undrained strength, $s_{u\text{-}n}/s_{u\text{-}in}$ (where $s_{u\text{-}n}$ - current undrained strength; $s_{u\text{-}in}$ – initial undrained strength), with increasing cycle number, n for Sample 1 (OCR = 1) and Sample 2 (OCR = 10), respectively, at two different distances below the T-bar pause depth. The subfigures (a) in both Figures 5 and 6 correspond to $s_{u\text{-}n}/s_{u\text{-}in}$ at a distance below the T-bar hold point (Δz) of approximately 0.4D (i.e. close to the centre of the cycles where the T-bar was held during wait periods in between

cyclic episodes), whereas subfigures (b) correspond to $s_{u\text{-}n}/s_{u\text{-}in}$ at $\Delta z = 1.4D$, which is close to the bottom of the

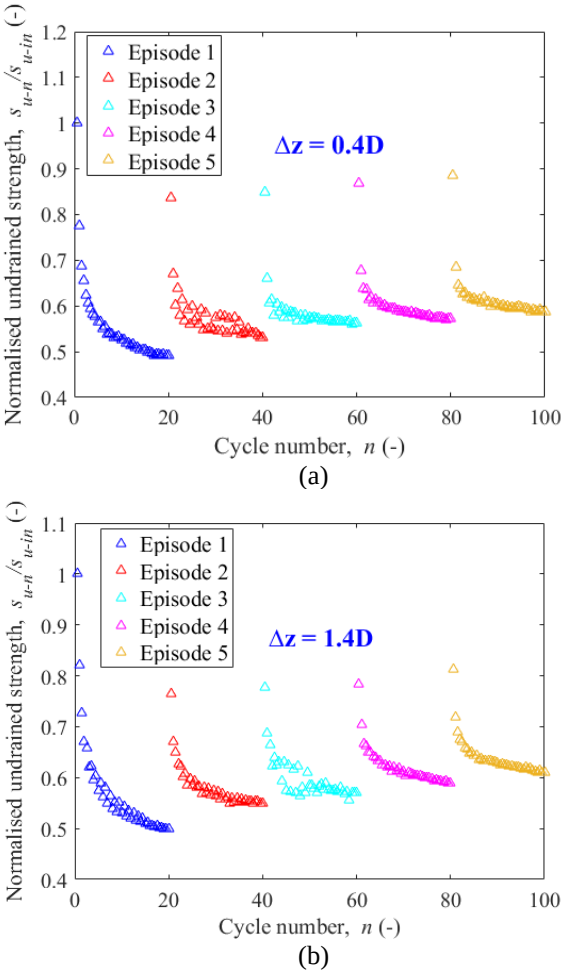

Figure 5. Change in undrained strength in Sample 1 (OCR = 1) extracted from: (a) 0.4D below the T-bar hold point; (b) 1.4D below the T-bar hold point

cyclic ranges. For clarity, the depths where these $s_{u\text{-}n}/s_{u\text{-}in}$ ratios were extracted are indicated in Figure 4.

Figures 5 and 6 indicate that for each episode, the $s_{u\text{-}n}$ decreases exponentially with cycles, in a manner similar to that decribed by Einav and Randolph [14]. In the first episode, a sensitivity (inverse of $s_{u\text{-}n}/s_{u\text{-}in}$ from the last cycle) of ~ 2 was measured in both Samples 1 and 2.

As can be seen in Figure 5(a), for Sample 1, the initial undrained strength following a pause period decreases by about 16% after the first episode but increases over later episodes, eventually achieving an initial strength that is about 90% of the original monotonic strength after 5 episodes. Close to the T-bar resting depth, the remoulded strength also increases (albeit slowly) with increasing number of episodes – with a total increase of about 20% relative to the initial remoulded strength. As observed in Figure 5(b), farther away from the hold point, the reduction in initial re-penetration resistance (relative to initial penetration) is larger, but the increasing trends of both the re-penetration and remoulded strengths remain in subsequent episodes.

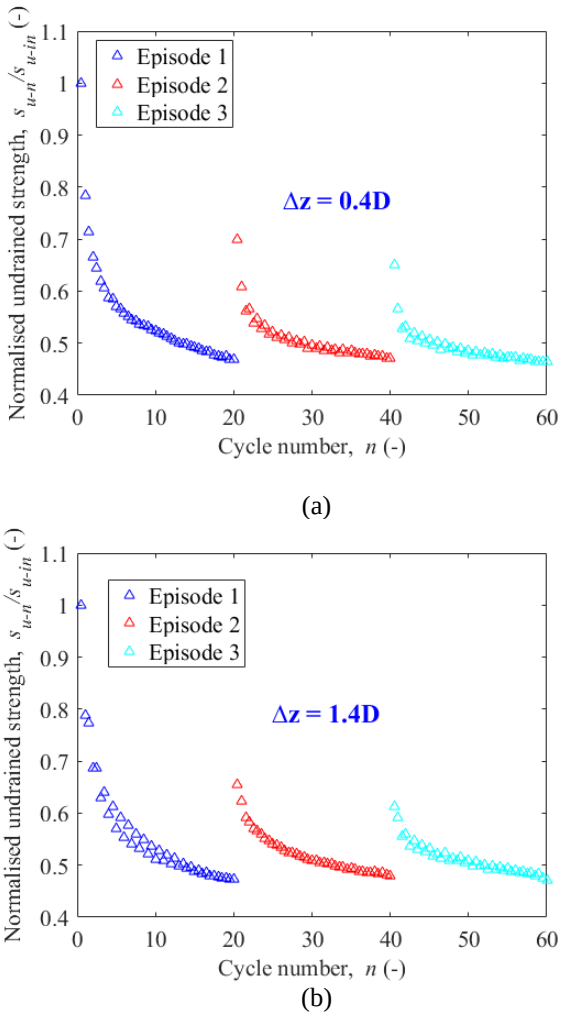

Figure 6. Change in undrained strength in Sample 2 (OCR = 10) extracted from: (a) 0.4D below the T-bar hold point; (b) 1.4D below the T-bar hold point

In constrast, for OCR = 10 (see Figure 6), there is no apparent increase in either the initial re-penetration resistance or the remoulded strength at both depths. In fact, the re-penetration strength and, to a lesser extent, the remoulded strength continue to reduce, suggesting that the soil is not densifying/getting stronger due to reconsolidation.

Clearly (from Figures 4 - 6), there is a spatial difference in the amount of strength changes that occur, depending on how close the soil is to the position where the T-bar remains stationary during wait periods. This observed behaviour was also evident in the episodic T-bar tests in kaolin clay as depicted in Figure 1, where the T-bar strength increase is greater close to the bottom-most extent of the cyclic displacement range – i.e. the position where the T-bar was held during wait periods.

From a theoretical perspective, in contractile, normally consolidated clays, the net excess pore pressure due to cyclic loading should be positive and pore water is expelled during reconsolidation, leading to soil void ratio reductions. Previous work has shown this to result in an increase in strength [3, 15, 16]. In contrast for overconsolidated clays, the net excess pore pressure is in theory, negative during (large amplitude) shearing. This would mean that during reconsolidation, water is drawn

into the soil pores, thereby causing the post-reconsolidation soil strength to decrease. These qualitative expectations based on critical state soil mechanics are generally consistent with the observerations of the current two tests.

However, the spatial differences in strength gain evident herein suggest that the boundary value problem may be complicated by the characteristics of the stresses applied by the T-bar to the soil. In order to properly quantify this effect, the overall stress (and the resulting strain) field around the T-bar should be considered in future research.

5. Comparison with kaolin clay

Although the current episodic T-bar tests in GoM clay showed differences in strength changes depending on the number of episodes and the state (stress history) of the soil, the level of strength gain observed for Sample 1 (OCR = 1) is relatively small. Much of the previous work conducted in this area has focused on the response of kaolin clay, which is commonly used in laboratory model testing and hence it is useful to compare the observed test results with those previously published for kaolin.

Figure 7 shows $s_{u\text{-}n}$ normalised by the initial monotonic strength ($s_{u\text{-}in}$) plotted versus dimensionless time $T = c_v t/D^2$ (instead of number of cycles) for both $s_{u\text{-}n}/s_{u\text{-}in}$ measured during initial T-bar re-penetration (Figure 7(a)) and at the last cycle (Figure 7(b)) for each episode. These are compared with kaolin clay results from White and Hodder [3], where both the initial re-penetration and remoulded (last cycle) $s_{u\text{-}n}/s_{u\text{-}in}$ in each episode is taken at a distance $\Delta z = 0.4D$ above the T-bar resting point, which was at bottom of the cyclic displacement range, as indicated in Figure 1(a). Here, the c_v was calculated as:

$$c_v = \frac{kE_o}{\gamma_w} \quad (3)$$

where E_o is the apparent stiffness in one-dimensional loading/unloading-reloading, taken here as $(1 + e)\sigma'_v/\lambda$ and $(1 + e)\sigma'_v/\kappa$ for Samples 1 (OCR = 1) and 2 (OCR = 10), respectively. The permeability, k for these samples were estimated from Equation 1. The λ and κ parameters for kaolin are 0.26 and 0.06 respectively [17]. The resulting estimated c_v for kaolin, Sample 1 and Sample 2 were 6.8 m^2/year, 1 m^2/year and 0.53 m^2/year, respectively. It can be seen here that the kaolin c_v is much larger, perhaps partly due to its higher silt content, which is reflected by its lower plasticity index (PI) of ~ 30% (compared with 73% for the GoM clay).

For kaolin (OCR ~ 1.8), broadly similar trends to that measured in Sample 1 were observed with increasing re-penetration peaks (see Figure 7(a)) as well as increasing remoulded strength (see Figure 7(b)) after waiting periods. Ignoring the $s_{u\text{-}n}/s_{u\text{-}in}$ in episode 1 for normally consolidated GoM clay (since there is a decrease in $s_{u\text{-}n}/s_{u\text{-}in}$ in episode 2 relative to that in episode 1); the rate of increases in both re-penetration and remoulded $s_{u\text{-}n}/s_{u\text{-}in}$ for kaolin are ~9 and 4 times larger (respectively) than that for the current tests in GoM clay. Similar to that observed in Figure 6(a), both the re-penetration and remoulded $s_{u\text{-}n}/s_{u\text{-}in}$ decrease after waiting periods for Sample 2 (OCR = 10).

These differences in strength changes may be attributed to differences in testing conditions between kaolin and the current GoM tests – e.g. the cyclic displacement ampltidue (45 mm in kaolin versus 20 mm in GoM), the absolute values of waiting times (3.5 versus 10 hours) or the position of the T-bar during the waiting times (bottom of the cycle versus midpoint). However, some insight into the differences in soils can be gained by comparing the ratio of κ/λ between the two soils. Since κ controls the change in void ratio as pore pressure dissipates and the ultimate change in undrained strength depends on λ, the κ/λ ratio should be proportional to the rate of strength evolution during reconsolidation [18]. For kaolin, $\kappa/\lambda = 0.23$ compared with $\kappa/\lambda = 0.1$ for GoM. The higher magnitudes of κ/λ (and c_v) for kaolin than that of the NC GoM sample may cause the differences in $s_{u\text{-}n}/s_{u\text{-}in}$ increase between the soils. Ascertaining how the differences in fundamental soil properties affects the rate and magnitude of strength increase in difference soils warrants further investigation.

6. Conclusions

The results presented provide insights into the factors that affect the potential for strength changes in normally consolidated and overconsolidated Gulf of Mexico (GoM) clay samples due to long term, large displacement T-bar cyclic tests. In particular, the stress history of the soil appears to have a significant effect on the occurrence of reconsolidation-induced strength changes.

In the normally consolidated sample, the undrained strength appears to increase with increasing cyclic episodes and this may be linked to reconsolidation-induced densification of the soil. In contrast, increasing levels of strength loss are apparent with increasing cyclic episodes in the highly overconsolidated sample, demonstrating that reconsolidation has an opposite effect (compared to normally consolidated soils) in dilatant soils.

This paper has also highlighted the potential link of the rate of strength gain to the fundamental consolidation properties of a given soil, where larger κ/λ ratios may yield higher rate of reconsolidation induced strength changes.

These findings highlight the need to account for the soil stress history in estimating the amount of strength change that may occur in soils (and associated geosystems) over service lifetimes. This is particular relevant for soil strength gain/loss with continuous cyclic loading when designing offshore infrastructure, especially that interacting with near seabed soils where variation in soil stress history is often the greatest. The findings in this paper may also have implications for laboratory testing, where samples prepared via application of dead weight, which are then removed for testing or via self-weight consolidation of a sample initially prepared at a low mositure content may have an induced overconsolidated soil profile. In these cases, overconsolidation may mask any potential strength increases that could occur in the field.

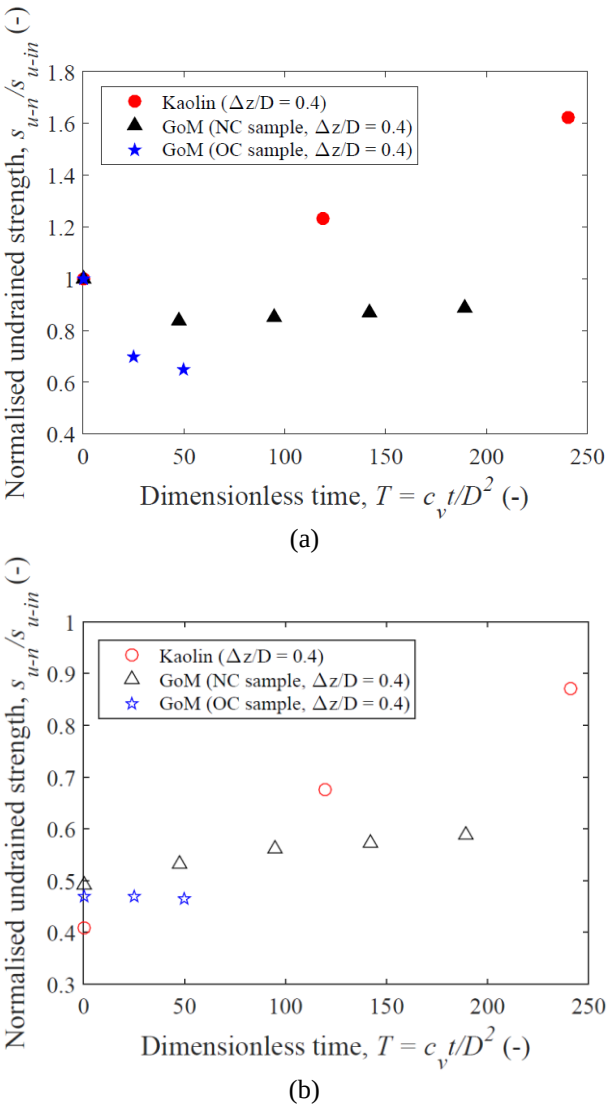

Figure 7. Change of $s_{u\text{-}n}/s_{u\text{-}in}$ during T-bar: (a) re-penetration; (b) last cycle with dimensionless time, T for kaolin [3] and GoM clays at a distance of Δz/D = 0.4 from where the T-bar was held during wait periods (see Figures 1 and 4)

Acknowledgements

The first and second authors are grateful for the postdoctoral financial support provided by the ARC Industrial Transformation Research Hub for Offshore Floating Facilities, which is funded by the Australian Research Council, Woodside Energy, Shell, Bureau Veritas and Lloyds Register (Grant No. IH140100012). The first author also acknowledges the financial support received from Universiti Malaysia Sarawak. The third author was supported by the Woodside OceanWorks internship programme during her visit to UWA to perform the testing described here. The fourth author is supported by the Shell Chair in Offshore Engineering and the fifth author is supported by the Fugro Chair. The test programme was performed at The National Geotechnical Centrifuge Facility at UWA and was supported by Manuel Palacios and Adam Stubbs. All support is gratefully acknowledged.

References

[1] Andersen, K. H., "Bearing capacity under cyclic loading—offshore, along the coast, and on land. The 21st Bjerrum Lecture presented in Oslo, 23 November 2007," *Canadian Geotechnical Journal*, vol. 46, no. 5, pp. 513-535, 2009.

[2] Zhou, Z., O'Loughlin, C. D., and White, D. J., "An effective stress analysis for predicting the evolution of SCR–seabed stiffness accounting for consolidation," *Géotechnique*, pp. 1-20, 2019.

[3] White, D. J. and Hodder, M., "A simple model for the effect on soil strength of episodes of remoulding and reconsolidation," *Canadian Geotechnical Journal*, vol. 47, no. 7, pp. 821-826, 2010.

[4] O'Loughlin, C. D., Zhou, Z., Stanier, S. A., and White, D. J., "Load-controlled cyclic T-bar tests: a new method to assess the combined effects of cyclic loading and consolidation," *Géotechnique Letters*, vol. 9, no. 4, 2019.

[5] Al-Khafaji, Z. A., Young, A. G., DeGroff, W., and Humphrey, G. D., "Geotechnical properties of the Sigsbee escarpment from deep soil borings," in *Offshore Technology Conference*, Houston, Texas, U.S.A, 2003: Offshore Technology Conference.

[6] Schroeder, K., Andersen, K. H., and Tjok, K. M., "Laboratory testing and detailed geotechnical design of the Mad Dog Anchors," in *Offshore Technology Conference*, Houston, Texas, U.S.A, 2006: Offshore Technology Conference.

[7] Al-Tabbaa, A. and Wood, D. M., "Some measurements of the permeability of kaolin," *Géotechnique*, vol. 37, no. 4, pp. 499-514, 1987.

[8] Chung, S. F., Randolph, M. F., and Schneider, J. A., "Effect of penetration rate on penetrometer resistance in clay," *Journal of Geotechnical and Geoenvironmental Engineering, ASCE*, vol. 132, no. 9, pp. 1188-1196, 2006.

[9] Randolph, M. F. and Hope, S., "Effect of cone velocity on cone resistance and excess pore pressures," in *Proceedings of the International Symposium on Engineering Practice and Performance of Soft Deposits*, Osaka, Japan, 2004.

[10] Martin, C. M. and Randolph, M. F., "Upper-bound analysis of lateral pile capacity in cohesive soil," *Geotechnique*, vol. 56, no. 2, pp. 141-145, 2006.

[11] Randolph, M. F. and Houlsby, G. T., "Limiting pressure on a circular pile loaded laterally in cohesive soil," *Geotechnique*, vol. 34, no. 4, pp. 613-623, 1984.

[12] Ladd, C., Foott, R., Ishihara, K., Schlosser, F., and Poulos, H. G., "Stress deformation and strength characteristics," in *Proceedings of the 9th International Conference on Soil Mechanics and Foundation Engineering*, Tokyo, 1977, vol. 2, pp. 421-494.

[13] Wroth, C., "The interpretation of in situ soil tests," *Géotechnique*, vol. 34, no. 4, pp. 449-489, 1984.

[14] Einav, I. and Randolph, M. F., "Combining upper bound and strain path methods for evaluating penetration resistance," *International Journal For Numerical Methods In Engineering*, vol. 63, pp. 1991-2016, 2005.

[15] Sahdi, F., White, D. J., and Gaudin, C., "Experiments using a novel penetrometer to assess the changing strength of clay during remolding and reconsolidation," *Journal of geotechnical and geoenvironmental engineering*, vol. 143, no. 4, pp. 1 - 7, 2017.

[16] Zhou, Z., White, D. J., and O'Loughlin, C. D., "An effective stress framework for estimating penetration resistance accounting for changes in soil strength from maintained load, remoulding and reconsolidation," *Géotechnique*, vol. 69, no. 1, pp. 57 - 71, 2018.

[17] Lehane, B. M., O'Loughlin, C. D., Gaudin, C., and Randolph, M. F., "Rate effects on penetrometer resistance in kaolin," *Géotechnique*, vol. 59, no. 1, pp. 41-52, 2009.

[18] Yan, Y., White, D. J., and Randolph, M. F., "Cyclic consolidation and axial friction for seabed pipelines," *Géotechnique Letters*, vol. 4, no. 3, pp. 165-169, 2014.